Experiments in Fluids 21 (1996) 118–123 © Springer-Verlag 1996

An experiment on the breakup of impinging droplets on a hot surface

Y. S. Ko, S. H. Chung

Abstract Breakup characteristics of liquid droplets impinging on a hot surface are investigated experimentally with the wall temperatures in the Leidenfrost temperature range of 220–330°C for n-decane fuel. Factors influencing droplet breakup are wall temperature, impinging velocity, droplet diameter and impinging angle. The 50% breakup probability shows that the impinging velocity decreases linearly with the droplet diameter increase and there exists an optimum impinging angle near 80° having the minimum value in the impinging velocity for given wall temperature and droplet size. Near the wall temperature of 250°C corresponding to the Leidenfrost temperature, a peculiar nonlinear behavior in the breakup probability is observed.

1 Introduction

The breakup of impinging droplets on a hot surface is an important phenomenon in such systems as a fuel injection in a diesel engine combustor, a sprinkler in a fire protection system, and a cooling system in continuous casting and rolling processes in metal sheet manufacturing. Especially, droplets impinging on a hot surface in a diesel combustor usually experience the wall temperature in the range of 240–300°C (Heywood 1988).

Droplet behavior on a hot surface exhibits typical Leidenfrost phenomenon (Tamura and Tanasawa 1959; Makino and Michiyoshi 1984; Cho and Law 1985; Xiong and Yuen 1991) when the wall temperature is approximately 100 K above the boiling point in hydrocarbon fuels, resulting in the levitation of the droplet over a hot surface by the ejection of vapor from the droplet surface. Based on the evaporation lifetime of a droplet with wall temperature variation, four different evaporation regimes can be identified; film evaporation, nucleate boiling, transition boiling and spheroidal vaporization (also called as film boiling). These regimes are identified for a stationary droplet on a surface (Tamura and Tanasawa 1959; Hsu and Graham 1976).

Studies accounting for the effect of a droplet impingement are relatively few. If one considers the effect of impinging velocity, especially interesting regimes in conjunction with the droplet dynamics are the transition boiling and film boiling regimes. Since, in other regimes, the droplet will wet and stay on the surface for most part of its vaporization period.

Recently, Anders et al. (1993) studied the behavior of impinging droplets by using a vibrating orifice type droplet generator with the typical generation frequency of 50 kHz. Various different kinds of droplet wall interactions are observed ranging from complete wetting to near elastic reflection of droplets depending on the wall temperature and impinging velocity. The formation of secondary droplets is also observed when the impinging velocity is high and the wall temperature is above the Leidenfrost temperature, however, the characteristics of breakup have not been extensively investigated.

Motivated by the importance of the breakup of impinging droplets on the droplet size distribution and cooling rate in diesel combustors or fire protection systems, the present study focuses on the breakup behavior accounting for the effects of droplet size, impinging velocity, impinging angle and wall temperature.

2 Experiment

Experimental setup consists of three parts including a droplet generation system, a surface heater and a visualization system, as schematically shown in Fig. 1. The droplet generation system has a pulse generator, a voltage amplifier, a droplet generator and a fuel reservoir. An electric pulse of 5 V with variable duty and frequency is generated from a PC-8253 card. Here, the duty is defined as the ratio of the duration maintaining 5 V to one period. The pulse is amplified to 20–140 V through the voltage amplifier.

The droplet generator is made of a cylindrical piezoelectric material (Edo Western, EC-65 II) with O.D. and I.D. of 12.7 mm and 10.2 mm, respectively, and the length of 25 mm. The amplified pulse with duty of 1/2 drives the droplet generator by contracting the piezoelectric cylinder. The stability, diameter and ejection velocity of the generated droplets are determined by various factors such as the pulse frequency, duty, voltage, nozzle diameter and shape, and the liquid fuel head between the nozzle and fuel reservoir. Fuel used is n-decane. The nozzle is made of quartz tube with I.D. 1.8 mm and the nozzle diameter is in the range of 300 μm. For the protection of the

Received: 22 May 1995/Accepted: 7 February 1996

Y. S. Ko, S. H. Chung
Department of Mechanical Engineering,
Seoul National University,
Seoul 151-742, Korea

Correspondence to: S. H. Chung

This work was supported by the Turbo and Power Machinery Research Center, Seoul National University.

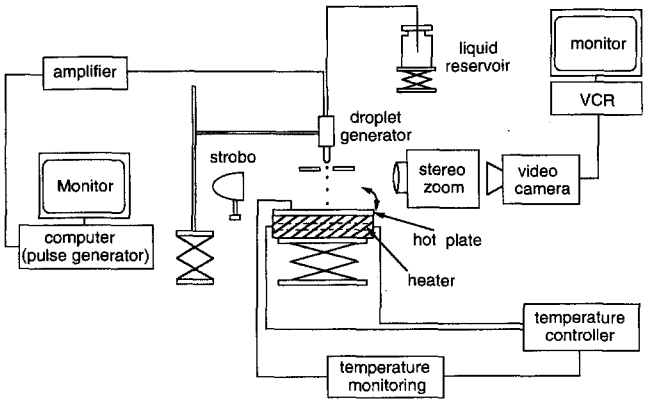

Fig. 1. Schematic diagram of experimental setup

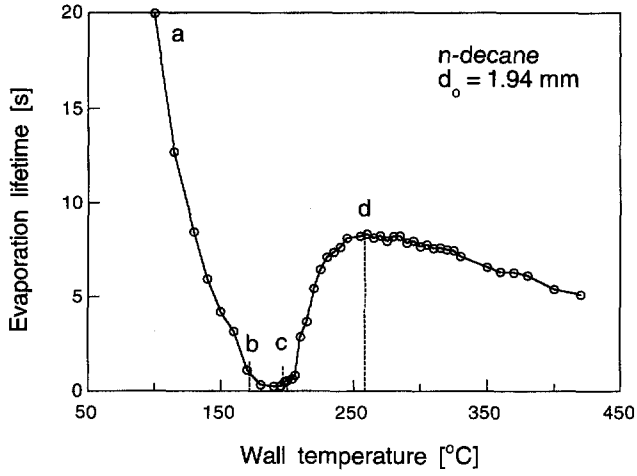

Fig. 2. The dependence of evaporation lifetime of n-decane droplet with wall temperature for $d_0 = 1.94$ mm

nozzle from the influence of a hot surface and for the stability of droplet generation, a circular shield with 7 mm hole is placed near the nozzle exit.

To minimize the local temperature drop near the impingement point by the successive bombardment of droplets, the present experiment is performed with the droplet generation frequency of 0.5 Hz in the breakup probability measurement, except for the visualization of droplet breakup where we use 50 Hz. The frequency of 0.5 Hz is several orders of magnitude lower than that of the vibrating orifice droplet generator, typically 50 kHz (Anders et al. 1993).

The surface heater consists of a mirror polished brass plate (230 mm × 30 mm × 3 mm) and a 750 W nichrome heater with a voltage and a temperature controller. A chromel–alumel thermocouple is used for the monitoring of wall temperature. The surface can be inclined from 90° to 45°, where 90° is defined as the normal collision of a droplet to the surface.

A stereozoom microscope, a video camera, a video tape recorder and a stroboscope are used for visualization. Impinging velocity and droplet size are measured at 3–5 mm above the surface from multiple exposure images with the shutter speed of 1/100 s and 300 Hz strobo. Droplet size is represented as an averaged value and the variation is within $\pm 3\%$. Impinging velocity is controlled by adjusting the fuel reservoir head and the position of the nozzle from the surface. For the visualization through the video recording, the generation frequency of droplets of 50 Hz is used. The stroboscope frequency is maintained slightly off from the generation frequency such that different phases of the impingement of consecutive droplets are recorded, thus having a similar effect as high speed visualization. The breakup probability, defined as the ratio of the number of droplet breakup after the collision with the hot surface to the total number of impingement, is measured by observing through the stereozoom microscope from the total number of 200–400 impinging droplets.

3
Results and discussions

A preliminary test of the evaporation characteristics of a droplet on a hot surface is conducted for the interpretation of the breakup behavior by the change in the wall temperature. Figure 2 shows the evaporation lifetime of n-decane fuel droplet having the initial diameter d_0 of 1.94 mm as a function of the wall temperature T_w. The droplet is placed on the surface by using a micro-syringe. The evaporation lifetime, defined as the duration from placing a droplet on the surface to complete vaporization, is averaged from the measurements using video images.

From this vaporization behavior, one can define several distinct temperatures. These are the boiling point of n-decane, 174.1°C, and temperatures corresponding to the local minimum and maximum in the evaporation lifetime. For $T_w <$ 174.1°C (point b corresponding to B.P.), the droplet is wetted on the surface and the evaporation lifetime rapidly decreases with the increase in the wall temperature.

The droplet is still wetted on the surface until the temperature reaches the point c (195°C), where the evaporation lifetime has the local minimum. Near the point c, several bubbles are formed and grow inside the droplet, resulting in a fragmentation of the droplet by the nucleate boiling between the droplet and the hot surface.

As the temperature further increases, the droplet is levitated by the balance of the evaporation momentum from the droplet surface and the gravity, showing the Leidenfrost phenomenon. Then, the evaporation lifetime is increased with increasing wall temperature until the critical point d (255°C) is reached. In the range of $195°C < T_w < 255°C$, the evaporation rate is reduced by the levitation, which has stronger effect than that of the enhancement of evaporation by the increase in the wall temperature.

For $T_w > 255°C$, the evaporation lifetime slowly decreases because of the enhancement of vaporization with the increase in the wall temperature. The region a–b corresponds to the film evaporation, b–c the nucleate boiling, c–d the transition boiling and after d the spheroidal vaporization.

The observation of the impinging droplets in the low temperature region is as follows. Near $T_w = 160°C$ which is below the boiling point, the droplet is wetted on the surface and is slowly vaporized without having a vapor film between the droplet and the surface. As the temperature increased to 190°C which is above the boiling point, the droplet on the surface shows irregular shapes and part of the liquid from the droplet is fragmented into small droplets. At 195°C, this

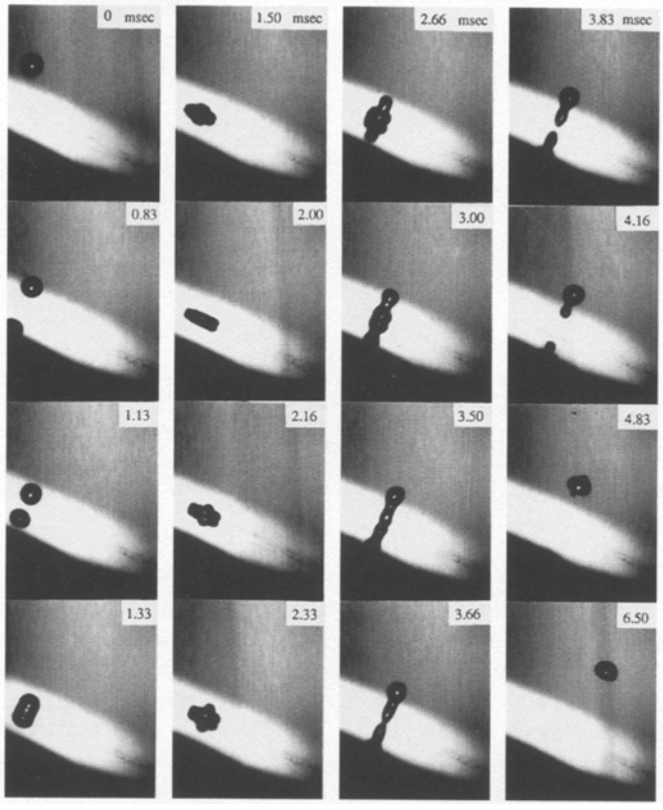

Fig. 3. Photographs showing droplet impinging process without breakup for $d_0 = 510$ μm, $T_w = 220°C$, $V = 0.83$ m/s and $\alpha = 60°$

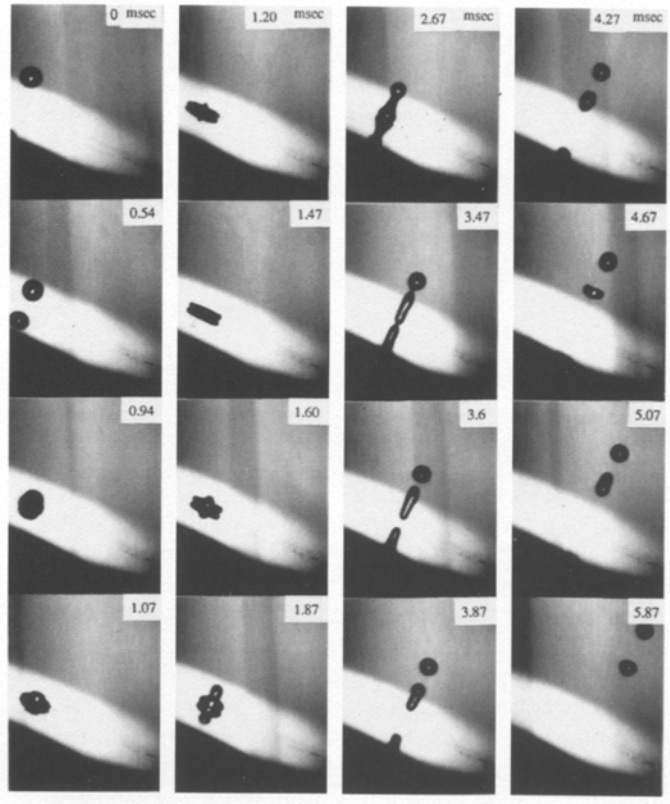

Fig. 4. Photographs showing droplet impinging process with breakup for $d_0 = 510$ μm, $T_w = 300°C$, $V = 0.79$ m/s and $\alpha = 60°$

phenomenon becomes more pronounced that fragmentation becomes vigorous, leading to the decrease in the evaporation lifetime. The generation of the fragmented small droplets is due to the nucleate boiling from the hot surface, since the liquid is in direct contact with the surface. Small bubbles from the surface grow and burst, thus generating small fragmented droplets. In this low wall temperature range, the impinging droplets adhere to the surface and exhibit breakup in somewhat randomly due to the nucleate boiling.

In the high temperature range, series of photographs of impinging droplet exhibit bouncing and breakup upon collision as shown in Figs. 3 and 4 for the initial droplet diameter $d_0 = 510$ μm and the impinging angle $\alpha = 60°$. These show regular behavior. Figure 3 is the case for $T_w = 220°C$ (the transition boiling regime) and the impinging velocity $V =$ 0.83 m/s. This impinging droplet is deformed on the surface in the form of a cylindrical disk upon impact. The decrease in the radius of curvature along the periphery of the cylindrical disk will increase the surface tension force which is expected to have a pumping effect leading to the rise of the center portion of the liquid. This rising momentum forms a waist between the center portion and the remainder of the liquid. Finally, the whole droplet bounces from the surface by the rising momentum, the surface force of the leading portion (upper waist) which pulls the trailing portion (lower waist), and the levitation force between the droplet and the surface. After the bouncing, the surface tension force deforms the droplet to a spherical shape. This case does not exhibit a breakup.

At higher wall temperature $T_w = 300°C$ in the spheroidal vaporization regime, Fig. 4 shows similar behavior as the case of Fig. 3 except that the upper portion from the waist can not hold the lower portion, leading to the breakup into two small droplets upon impingement. The impinging velocity of $V = 0.79$ m/s in this case is even lower than that of Fig. 3. It is to be noted that the first bouncing droplet has near spherical shape while the second droplet is initially much elongated when it takes off from the surface. Then, the elongated droplet oscillates and has damping towards a spherical shape. This change in the breakup behavior with wall temperature can be attributed to several factors; the reduction in the surface tension by the rapid droplet heating from the hot surface and the recoiling effect by the rapid vapor ejection on the contact surface as the wall temperature increases.

Figure 5 shows the trajectories of droplet(s) corresponding to the case of Fig. 4. The points indicate the geometrical center of the spherical or elongated droplets. The impinging droplet with $\alpha = 60°$ is bounced and broken up into two droplets. The extended line of the trajectory of the first bouncing droplet nearly coincides with the central contacting point of the impinging droplet. The bouncing angles of these two droplets are slightly larger than the impinging angle, in this case near 65°. The droplets maintain nearly axisymmetric shapes upon collision and the effect of gravity is to reduce the bouncing angle. Even though, there is an overall momentum loss by the contact with the surface and by the deformation, one possible mechanism of increasing the bouncing angle is the normal

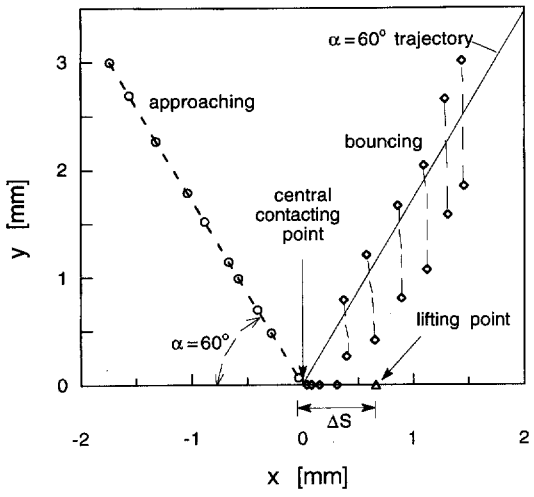

Fig. 5. The trajectory of impinging droplet with $T_w=300°C$, $d_0=510$ μm, $\alpha=60°$ (slip distance, $\Delta S=660$ μm)

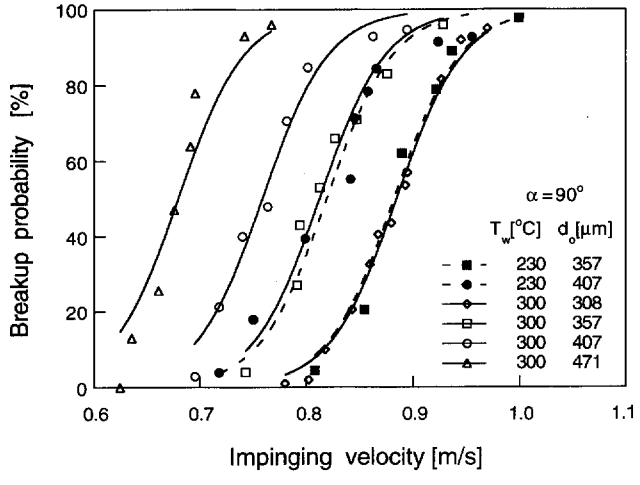

Fig. 6. Effect of impinging velocity and droplet size on droplet breakup probability for $\alpha=90°$

force exerted on the bouncing droplet by the vapor ejection on the contacting surface with the hot plate.

The second droplet shows a significant slip along the surface. The slip distance, defined as the distance from the central contacting point to the complete liquid lifting point, is 660 μm which is larger than the initial droplet diameter. The two bounced droplets are nearly in vertical positions to the surface, especially as they move away from the surface.

To investigate the characteristics of breakup, we have counted the breakup probability by varying the impinging velocity, impinging angle, wall temperature and droplet size. Figure 6 shows the breakup probability by varying the impinging velocity and droplet size for $\alpha=90°$ and $T_w=230°C$ and 300°C. For specified T_w and d_0, the breakup probability sharply increases from 0 to 100% as the impinging velocity increases. It also shows that the breakup is more difficult to occur for smaller droplet and the breakup is difficult for $T_w=230°C$ compared to the case for 300°C. The effect of wall temperature will be discussed in detail later.

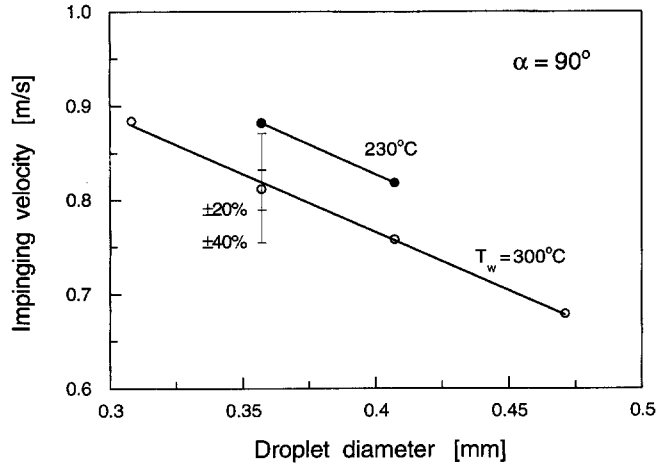

Fig. 7. The droplet diameter and impinging velocity relation at 50% breakup probability for $\alpha=90°$

Probability, in general, can be represented as a normal probability integral or an error function. In such a case, 50% probability can be used as a criterion in identifying a parameter dependence. Since, a hyperbolic tangent function can reasonably represent the similar functional behavior as the error function and yet does not contain integration, the present breakup probability is fitted in the form of tanh $a(x+b)$ where a and b are constants. For specified wall temperature, each data with constant droplet size are fitted, thus b values are determined for each droplet diameter. Using these b values, a is refitted to have a representative value irrespective of d_0.

The 50% breakup probabilities, thus determined, are shown in Fig. 7 to identify the effect of impinging velocity. It demonstrates that the impinging velocity decreases linearly with the droplet diameter increase in the range of $d_0=300$–500 μm. This behavior can be compared to the Weber number criteria for the breakup of free droplets, which is $We=\rho d_0 V^2/\sigma$ where ρ is the density and σ the surface tension. For free droplets, the breakup condition of constant Weber number is $V\propto d_0^{-1/2}$ since ρ and σ are constants for a specified condition.

For the present impinging droplets, the variation of density by droplet heating is expected to be relatively weak, while the surface tension varies significantly by heat transfer from the hot surface. For example, the density and the surface tension variations for n-decane are 1.2% and 5.9%, respectively, for the change of temperature from 100°C to 110°C (American Petroleum Institute 1971). For impinging droplets, the impinging velocity V and the droplet diameter d_0 affect impact dynamics, i.e., the deformation and thereby the droplet heating. As the impinging velocity increases, the droplets will be deformed more such that the droplet will have larger contact area with the hot surface and have longer time of contact, resulting in a much increased heat transfer. This influences the surface tension and also the momentum by the vapor ejection from the contact surface. The resultant effect exhibits the linear decrease in the impinging velocity with the increase in the droplet diameter for the breakup to occur.

The effect of impinging angle on the breakup probability for $T_w=300°C$ is shown in Fig. 8 as a function of impinging

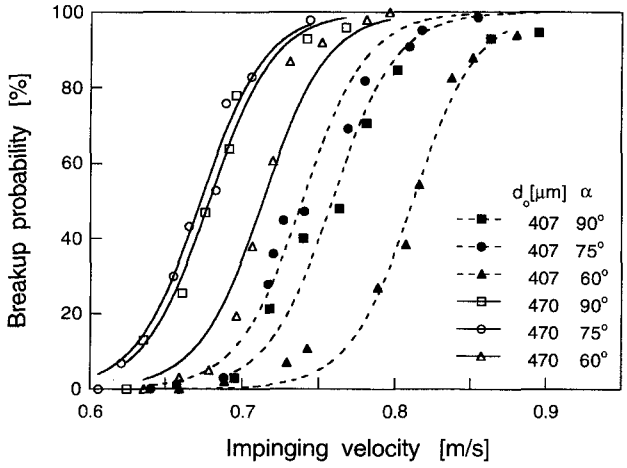

Fig. 8. Effect of impinging velocity and impinging angle on breakup for $T_w = 300°C$

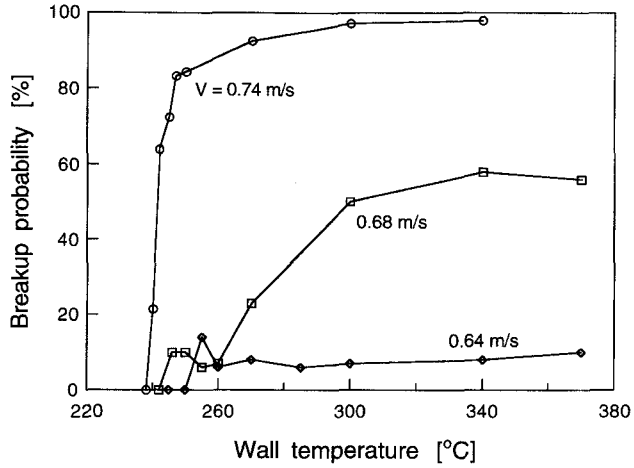

Fig. 10. Dependence of wall temperature on breakup probability for $d_0 = 470$ μm and $\alpha = 90°$

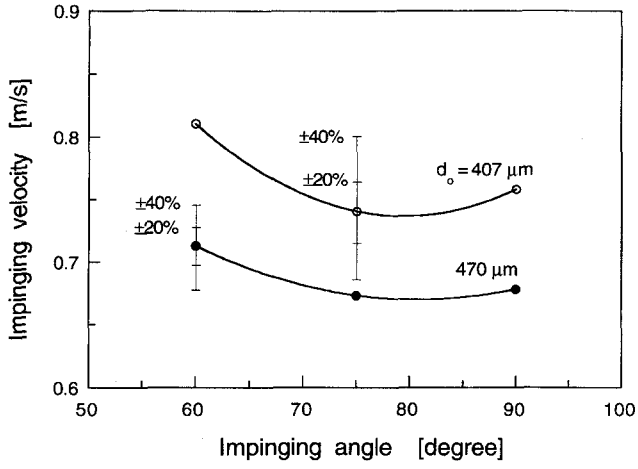

Fig. 9. The impinging angle and impinging velocity relation at 50% breakup probability for $T_w = 300°C$

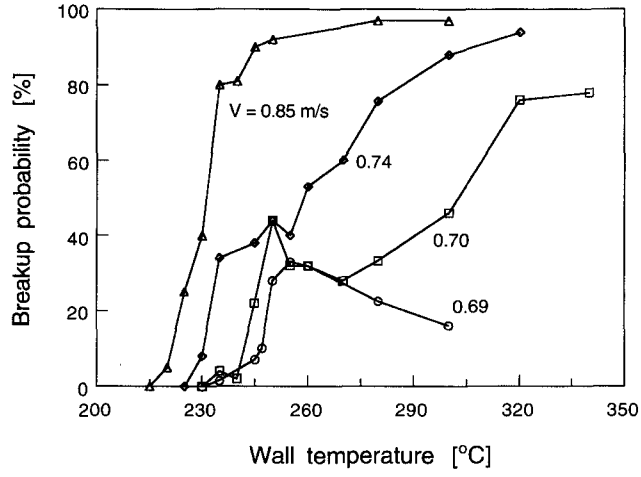

Fig. 11. Dependence of wall temperature on breakup probability for $d_0 = 470$ μm and $\alpha = 60°$

velocity. The overall shape of the breakup probability can also be reasonably represented as the hyperbolic tangent functions even though some deviations are demonstrated. For example, the range of impinging velocity for the change in the breakup probability from 0 to 100% for $\alpha = 60°$, is narrower compared to those for $\alpha = 75°$ and 90° for $d_0 = 470$ μm.

The peculiar aspect is the nonlinear dependence on the impinging angle, that is, $\alpha = 75°$ has consistently higher breakup probability than $\alpha = 90°$ and 60° for $d_0 = 407$ μm droplets by the variations in impinging velocity, and $d_0 = 470$ μm also shows similar behavior. This behavior is clearly demonstrated in Fig. 9 for the 50% breakup probability, showing an optimal impinging angle for breakup near $\alpha = 80°$.

The wall temperature can play a dominant role in affecting the breakup probability, since it is directly associated with the Leidenfrost phenomenon and the surface tension. Figures 10 and 11 represent the breakup probability as a function of wall temperature for various impinging velocities. Figure 10 is the case for $d_0 = 470$ μm and $\alpha = 90°$. In the high temperature region of $T_w > 300°C$, the breakup probability is not affected much by the wall temperature. On the other hand, it is a sensitive function of impinging velocity and wall temperature in the temperature range of $250 < T_w < 260°C$. The breakup probability for $V = 0.64$ m/s is even higher than that for $V = 0.68$ m/s. And also for $V = 0.64$ and 0.68 m/s, the breakup probabilities have local maxima near the wall temperature of 250°C.

These local maxima have been further demonstrated in Fig. 11 for $\alpha = 60°$, especially for low impinging velocities of 0.69 and 0.70 m/s. These nonlinear behavior also occurs in the vicinity of $T_w = 250°C$, which corresponds to the point of local maximum in the evaporation lifetime as exhibited in Fig. 2.

To further demonstrate the Leidenfrost effect on the breakup probability, we have plotted the breakup probability as a function of impinging velocity at various wall temperatures in Fig. 12. It clearly shows that the breakup probability can be reasonably represented as the normal probability integral except for $T_w = 250°C$, which shows the peculiar nonlinear behavior with impinging velocity that the lower impinging

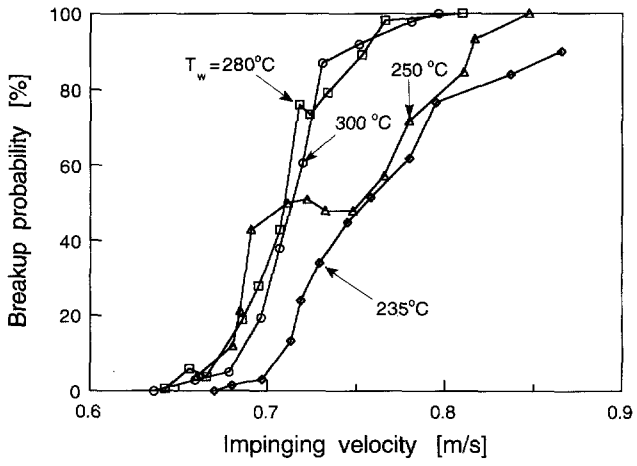

Fig. 12. Effect of wall temperature and impinging velocity on breakup probability for $d_0 = 470$ μm and $\alpha = 60°$

velocity has higher breakup probability in the range of 0.70–0.77 m/s.

4 Concluding remarks

The breakup behavior for n-decane fuel droplet impinging on a hot surface is studied experimentally including the effects of wall temperature, impinging velocity, droplet size and impinging angle. Details of the breakup process are observed and the importance of the wall temperature on breakup has been demonstrated. The impinging velocity linearly decreases with the droplet diameter increase for the 50% breakup probability. It is found that there exists an optimum impinging angle near 80° having the minimum impinging velocity. Wall temperature variation shows a peculiar nonlinear behavior in the breakup probability, especially near 250°C which corresponds to the temperature of local maximum droplet lifetime in the Leidenfrost phenomenon for n-decane.

The breakup mechanism of impinging droplet is a complex coupled phenomenon including the effect of impinging momentum, the deformation to an oblate shape, the effect of heat transfer to droplet, the effect of levitating force due to the ejection of vapor, the surface tension affecting the formation of a initial bouncing droplet, the formation of waist and the pumping force from the leading droplet to the liquid under the waist. The wall temperature, droplet size, impinging angle and impinging velocity are all coupled to the above mentioned effect. For example, the wall temperature affects the levitation force in Leidenfrost phenomenon and the surface tension. Further study is needed in fully explaining the breakup mechanism of impinging droplets on a hot surface.

References

American Petroleum Institute, Research Project 44 (1971) Selected Values of Properties of Hydrocarbons and Related Compounds. Thermodynamic Research Center, Texas A & M University

Anders K; Roth N; Frohn A (1993) The velocity change of ethanol droplets during collision with a wall analysed by image processing. Exp Fluids 15: 91–96

Cho P; Law CK (1985) Pressure/temperature ignition limits of fuel droplet vaporizing over a hot plate. Int. J. Heat Mass Transfer 28: 2174–2176

Heywood JB (1988) Internal combustion engine fundamentals. McGraw-Hill 698–700

Hsu YY; Graham RW (1976) Transport processes in boiling and two-phase systems. Hemisphere Publ 71—97

Makino K; Michiyoshi I (1984) The behavior of a water droplet on heated surfaces. Int. J. Heat Mass Transfer 27: 781–791

Tamura Z; Tanasawa Y (1959) Evaporation and combustion of a drop contacting with a hot surface. Seventh Symposium (International) on Combustion. The Combustion Institute, Pittsburgh, 509–522

Xiong TY; Yuen MC (1991) Evaporation of a liquid droplet on a hot plate. Int. J. Heat Mass Transfer 34: 1881–1894.